

Carbon Nanotube-Supported Dendritic Pt-on-Pd Nanostructures: Growth Mechanism and Electrocatalytic Activity Towards Oxygen Reduction

Sourov Ghosh, Siniya Mondal and C. Retna Raj*
Department of Chemistry, Indian Institute of Technology Kharagpur
Kharagpur 721302, India
E-mail: crraj@chem.iitkgp.ernet.in

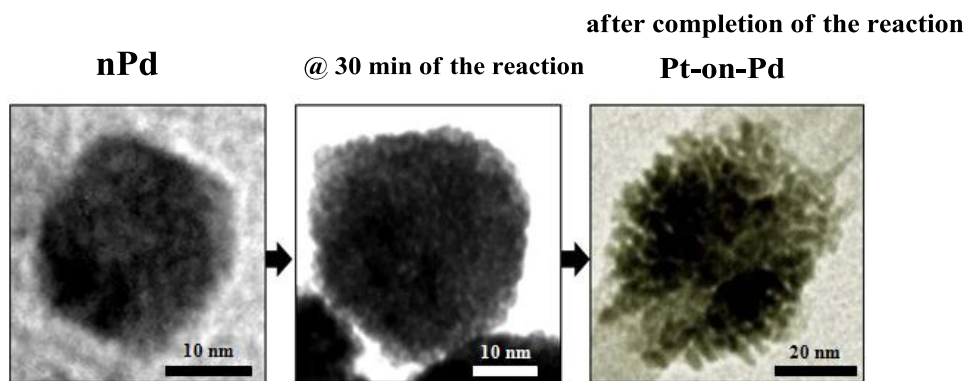
Table S1

The diffraction parameters obtained from the XRD profile of the different electrocatalyst.

Catalyst	$2\theta_{(111)}$	$2\theta_{(200)}$	$2\theta_{(220)}$	$2\theta_{(311)}$	$2\theta_{(222)}$
Only Pt	39.95	46.51	67.86	81.86	86.37
Pt₆₄Pd₃₆	39.96	46.51	67.89	81.89	86.47
Pt₅₂Pd₄₈	40.018	46.48	67.92	81.91	86.47
Pt₂₁Pd₇₉	40.03	46.58	67.96	81.98	86.56
Only Pd	40.05	46.61	68.01	81.98	86.56

Figure S1

Possible growth mechanism of Pt-on-Pd nanodendrites was investigated by TEM measurement. The size, shape and morphology of the initial Pd nanoparticle gradually changes during the growth of Pt dendrites over the Pd nanoparticles.



Average size: nPd ~22 nm

Pt-on-Pd at 30 min of the reaction: ~40 nm

Pt-on-Pd after the completion of the reaction: ~55 nm

Figure S2

UV-vis spectra illustrating the absence of galvanic displacement reaction between Pt(II) complex and Pd nanoparticles in the presence of DHA.

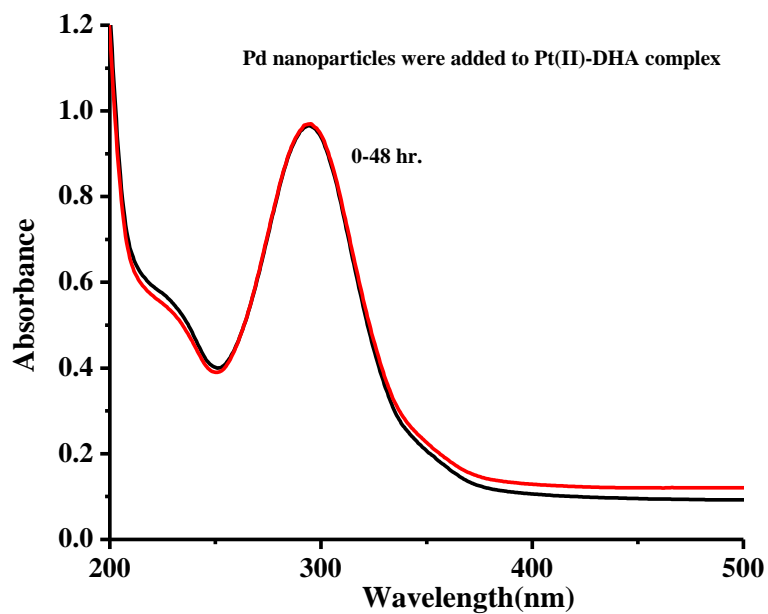


Figure S3

XRD profile for the MWCNT-supported Pt, Pd and Pt-Pd bimetallic nanostructures.

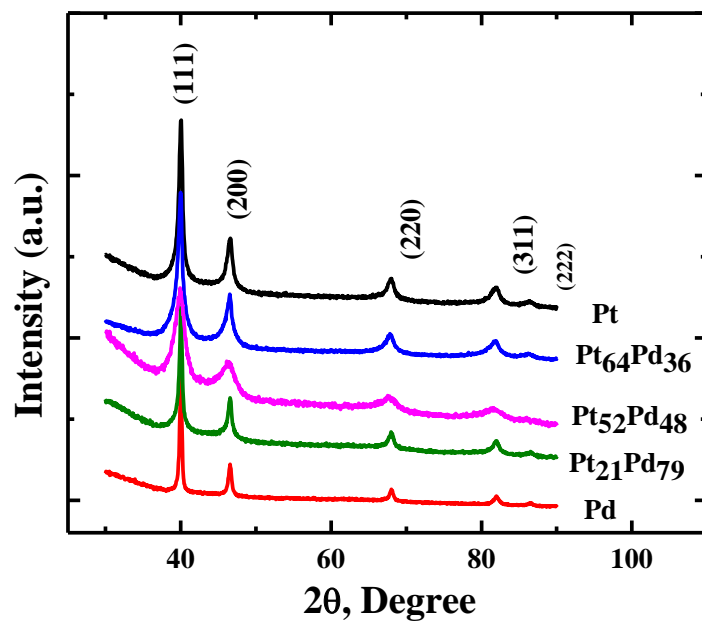


Figure S4

TEM images of MWCNT supported Pt (a) and Pd (b) nanoparticles.

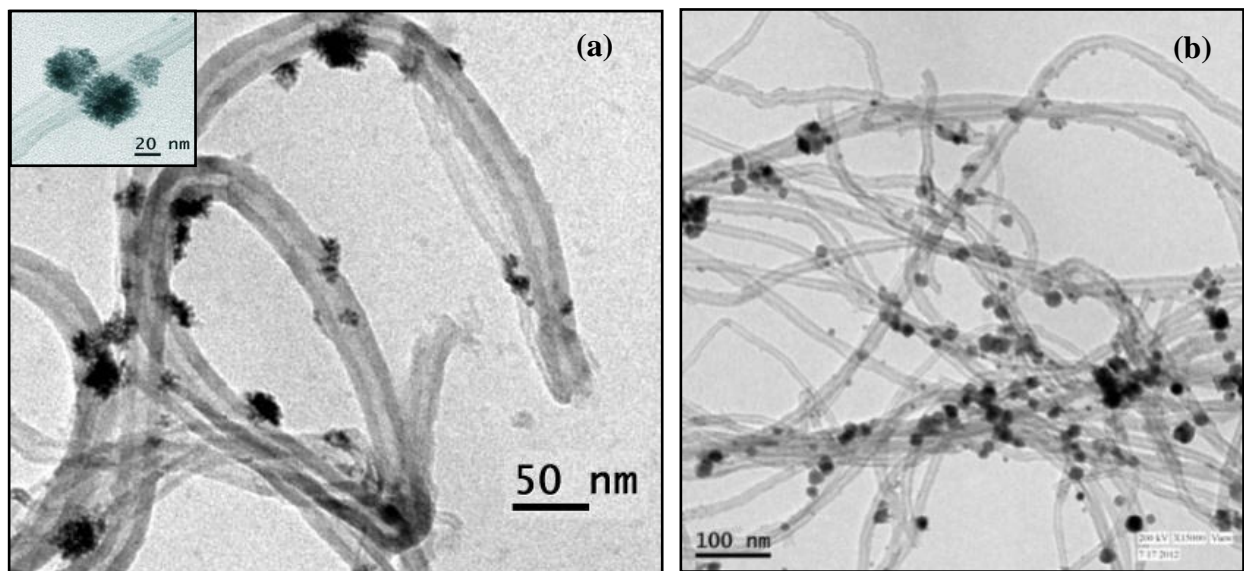


Figure S5

Energy dispersive spectral profile of the nanoparticles obtained at an intermediate stage of the synthesis of Pt₆₄Pd₃₆.

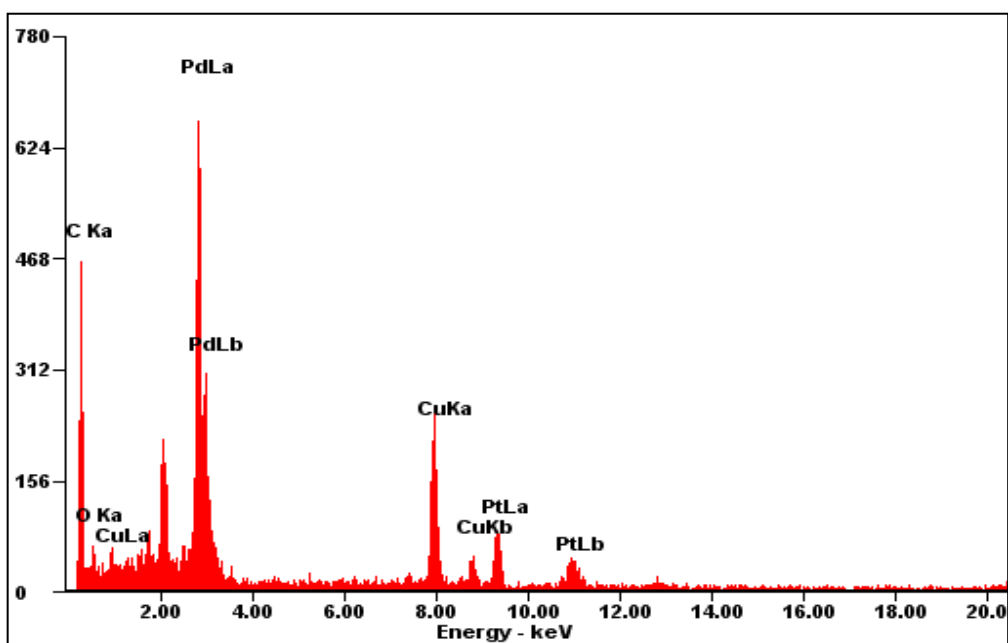


Figure S6

Cyclic voltammetric profile of Pt₆₄Pd₃₆, Pt₅₂Pd₄₈, Pt₂₁Pd₇₉ and Pt electrocatalyst-modified electrode in 0.5 M H₂SO₄. Scan Rate: 100mV/s.

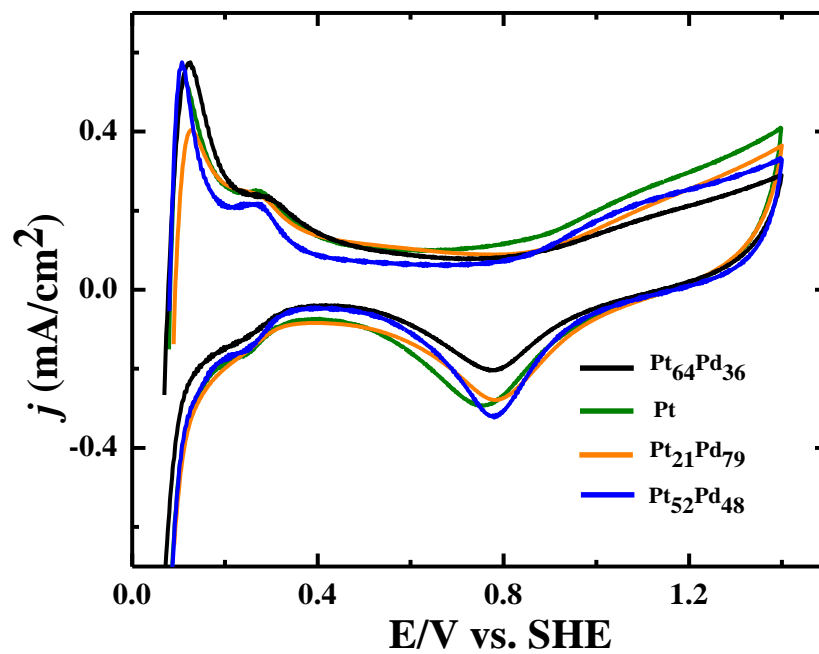


Figure S7

Rotation-dependent polarization curves for ORR on Pt₆₄Pd₃₆nanoparticles decorated MWCNT modified electrode in 0.5 M H₂SO₄. Scan rate: 5 mV/s. Ring potential: 0.85 V. The limiting current is normalized with geometrical surface area of the electrode.

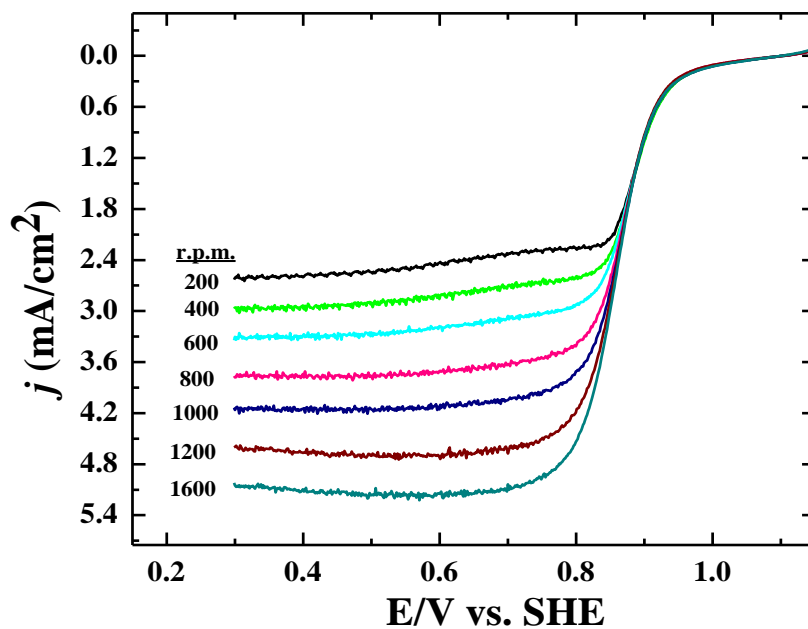


Figure S8

Plot illustrating the area specific activity of different catalyst towards ORR at the potential of 0.9 V.

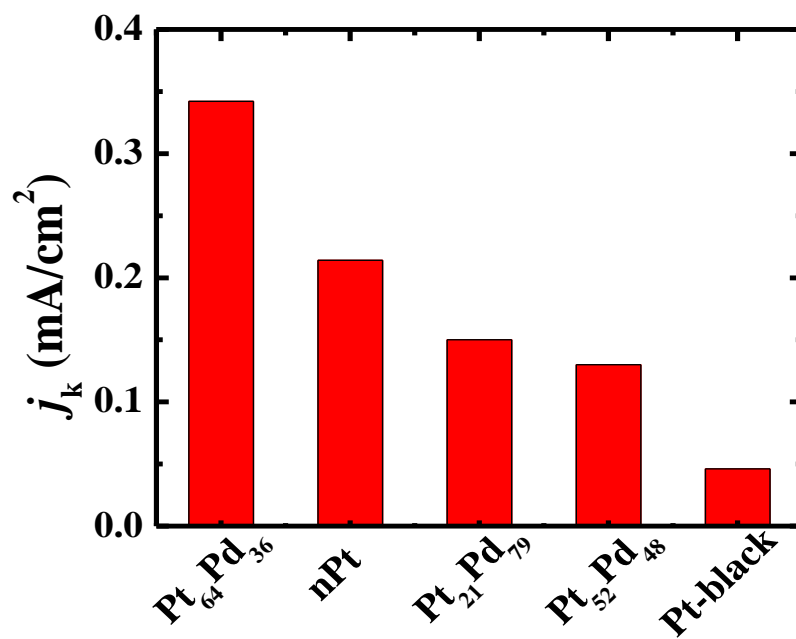


Figure S9

Figure illustrating the change of specific activity of different catalyst with respect to the Pt content.

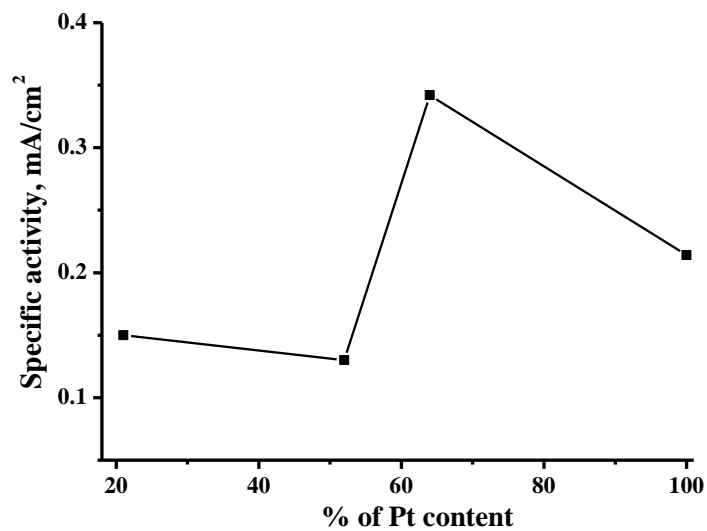


Figure S10

Plot illustrating the durability of different electrocatalyst towards oxygen reduction during extensive potential sweep.

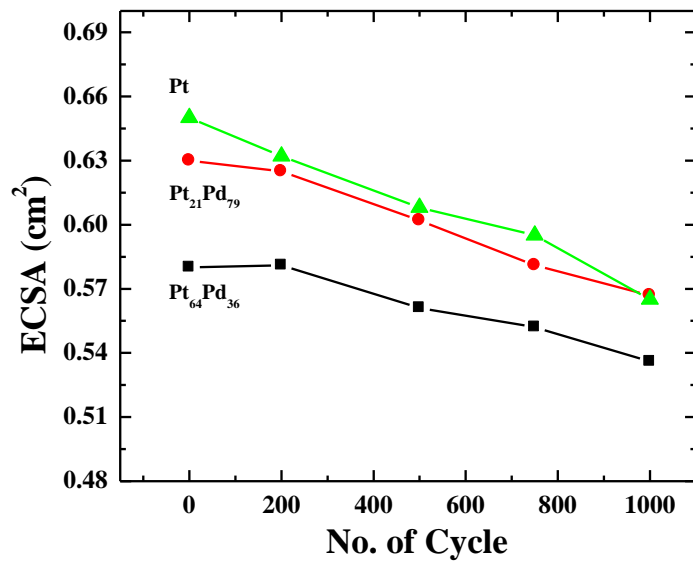


Figure S11

Polarization curve illustrates the durability of (A) Pt₂₁Pd₇₉/MWCNT and (B) Pt/MWCNT electrocatalyst after 1000 potential sweep. Electrolyte: 0.5 M H₂SO₄. Rotation rate: 800 rpm. Scan rate: 5 mV/s. Ring potential: 0.85 V. The limiting current is normalized with the geometric surface area of the electrode.

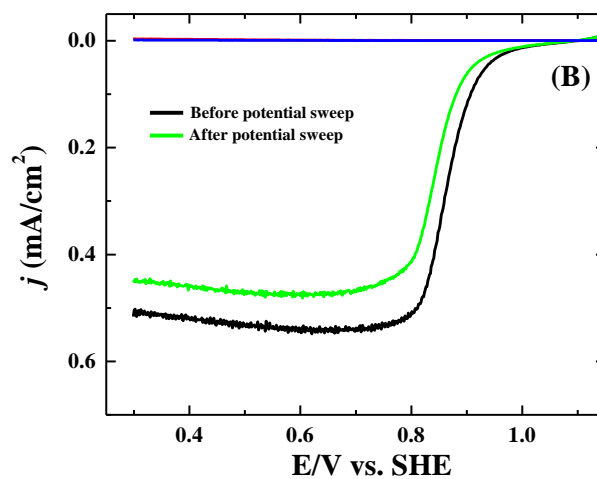
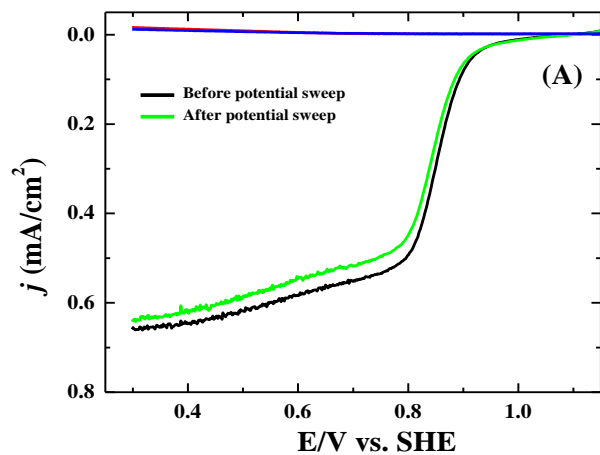


Figure S12

Cyclic voltammograms illustrating the poor durability of nPd-based electrode during ORR in sulfuric acid solution. Scan rate: 50 mV/s. The experiment was performed in oxygen saturated. The solution was saturated with oxygen before each sweep.

